Anisotropic electro-osmotic flow over superhydrophobic surfaces

Citation: Bahga, Supreet S., Olga I. Vinogradova, and Martin Z. Bazant. "Anisotropic electro-osmotic flow over super-hydrophobic surfaces." Journal of Fluid Mechanics 644 (2010): 245. © Cambridge University Press 2010

As Published: http://dx.doi.org/10.1017/S0022112009992771

Publisher: Cambridge University Press

Persistent URL: http://hdl.handle.net/1721.1/60963

Version: Final published version: final published article, as it appeared in a journal, conference proceedings, or other formally published context

J. Fluid Mech. (2010), *vol.* 644, *pp.* 245–255.
doi:10.1017/S0022112009992771

Anisotropic electro-osmotic flow over super-hydrophobic surfaces

SUPREET S. BAHGA,[1] OLGA I. VINOGRADOVA[2] AND MARTIN Z. BAZANT[1,3]†

[1]Department of Mechanical Engineering, Stanford University, Stanford, CA 94305, USA

[2]A. N. Frumkin Institute of Physical Chemistry and Electrochemistry, Russian Academy of Sciences, 31 Leninsky Prospect, 119991 Moscow, Russia

[3]Departments of Chemical Engineering and Mathematics, Massachusetts Institute of Technology, Cambridge, MA 02139, USA

(Received 13 July 2009; revised 14 October 2009; accepted 14 October 2009)

Patterned surfaces with large effective slip lengths, such as super-hydrophobic surfaces containing trapped gas bubbles, have the potential to greatly enhance electrokinetic phenomena. Existing theories assume either homogeneous flat surfaces or patterned surfaces with thin double layers (compared with the texture correlation length) and thus predict simple surface-averaged, isotropic flows (independent of orientation). By analysing electro-osmotic flows over striped slip-stick surfaces with arbitrary double-layer thickness, we show that surface anisotropy generally leads to a tensorial electro-osmotic mobility and subtle, nonlinear averaging of surface properties. Interestingly, the electro-osmotic mobility tensor is not simply related to the hydrodynamic slip tensor, except in special cases. Our results imply that significantly enhanced electro-osmotic flows over super-hydrophobic surfaces are possible, but only with charged liquid–gas interfaces.

1. Introduction

The development of microfluidics has motivated interest in manipulating flows in very small channels, which exhibit huge hydrodynamic resistance to pressure-driven flow (Stone, Stroock & Ajdari 2004; Squires & Quake 2005). One avenue for driving flow on such scales is to exploit hydrodynamic slip, usually quantified by the slip length b (the distance within the solid at which the flow profile extrapolates to zero) (Vinogradova 1999; Bocquet & Barrat 2007; Lauga, Brenner & Stone 2007). For hydrophobic smooth and homogeneous surfaces, b can be of the order of tens of nanometres (Vinogradova & Yakubov 2003; Cottin-Bizonne *et al.* 2005; Vinogradova *et al.* 2009), but not much more. Since the efficiency of hydrodynamic slippage is determined by the ratio of b to the scale of the channel h (Vinogradova 1995), it is impossible to benefit from such a nanometric slip for pressure-driven microfluidic applications.

In principle, this limitation does not apply to interfacially driven flows, such as electro-osmosis past a charged surface in response to an applied electric field. The combination of these two strategies can yield considerably enhanced electro-osmotic (EO) flow on hydrophobic surfaces (Muller *et al.* 1986; Joly *et al.* 2004; Ajdari &

† Email address for correspondence: bazant@mit.edu

Bocquet 2006), even for nanometric slip lengths. The reason is that the thickness of the electric Debye layer (EDL), characterized by the Debye screening length $\lambda_D = \kappa^{-1}$, defines an additional length scale of the problem, comparable to b. For a small surface charge density q, simple arguments show that the electro-osmotic mobility M_e, which relates the effective electro-osmotic slip velocity (outside the double layer) to the tangential electric field $u_s = M_e E_t$, is given by (Muller *et al.* 1986; Joly *et al.* 2004)

$$M_e = -\frac{\varepsilon\zeta}{\eta}(1 + b\kappa) = -\frac{q}{\eta\kappa}(1 + b\kappa), \tag{1.1}$$

where ε and η are the permittivity and viscosity of the solution, respectively, and $\zeta = q/\kappa\varepsilon$ is the zeta potential across the diffuse (flowing) part of the double layer. The factor $(1+b\kappa)$ associated with hydrodynamic slip can potentially enhance interfacially driven flow in microfluidic devices (Ajdari & Bocquet 2006), electrophoretic mobility of particles (Khair & Squires 2009) and electrokinetic energy conversion (streaming potential) in nanochannels (van der Heyden *et al.* 2006).

For this reason, it is attractive to consider electro-osmotic flows over superhydrophobic (SH) surfaces, whose texture on a scale L can significantly amplify hydrodynamic slip due to gas entrapment (Vinogradova *et al.* 1995; Cottin-Bizonne *et al.* 2003) leading to effective b of the order of several microns in pressure-driven flows (Ou & Rothstein 2005; Joseph *et al.* 2006). Equation (1.1) with $b\kappa \gg 1$ suggests that a massive amplification of EO flow can be achieved over SH surfaces, but the controlled generation of such flows is by no means obvious, since both the slip length and the electric charge distribution on an SH surface are inhomogeneous and often anisotropic. Despite its fundamental and practical significance, EO flow over SH surfaces has received little attention. Recently, Squires (2008) investigated EO flow past inhomogeneously charged, flat slipping surfaces in the case of thick channels ($h \gg L$) and thin EDL ($\lambda_D \ll L$) and predicted negligible flow enhancement in the case of an uncharged liquid–gas interface, which has been confirmed by molecular dynamics simulations (Huang *et al.* 2008). However, this work cannot be trivially extended to the general case of thick EDL ($\lambda_D \gg L$), where improved efficiency of electrokinetic energy conversion is expected (van der Heyden *et al.* 2006). For thick EDL, we might also expect anisotropic EO flows transverse to the applied electric field, as in the case of rough, no-slip charged surfaces (Ajdari 2001).

In this paper, we provide analytical solutions to electro-osmotic flows over weakly charged, textured slipping surfaces. We show that the electro-osmotic mobility is generally a tensorial property of the surface, reflecting nonlinear averaging of the slip length and charge profiles, and is not trivially related to the hydrodynamic slip tensor (Bazant & Vinogradova 2008). In § 2, we give basic principles, formulate the problem and obtain general solutions to longitudinal and transverse textures. Effective slip lengths and exact solutions to EO velocity over stick-slip stripes modelling SH surfaces are derived in § 3. Implications for the use of SH surfaces to enhance EO flows are discussed in § 4, followed by concluding remarks in § 5.

2. General theory

2.1. *Interfacial mobility tensor*

Ajdari (2001) pointed out that linear electrokinetic phenomena are generally tensorial in space and showed that microchannels with both charge and height variations can exhibit transverse electrokinetic effects. Here, we ascribe analogous behaviour to a 'thin interface', whose thickness λ is much smaller than the geometrical scale h, by

defining a tensorial electro-osmotic mobility via $\boldsymbol{u}_s = \boldsymbol{M}_e \boldsymbol{E}$, where $\boldsymbol{E}$ is the electric field and $\boldsymbol{u}_s$ is the effective fluid slip velocity just outside the interface (relative to the surface velocity). This is analogous to the tensorial hydrodynamic mobility $\boldsymbol{M}_h$, defined by $\boldsymbol{u}_s = \boldsymbol{M}_h \boldsymbol{\tau}$ in terms of the normal traction $\boldsymbol{\tau} = \hat{\boldsymbol{n}} \cdot \boldsymbol{\sigma}$, or equivalently, to the slip-length tensor $\boldsymbol{b} = \boldsymbol{M}_h \eta$ defined by $\boldsymbol{u}_s = \boldsymbol{b}\dot{\boldsymbol{\gamma}}$ for a Newtonian fluid, where $\dot{\boldsymbol{\gamma}} = \boldsymbol{\tau}/\eta$ is the strain rate (Bazant & Vinogradova 2008). We combine these effects in a general 'interfacial constitutive relation'

$$\begin{pmatrix} \boldsymbol{u}_s \\ \boldsymbol{j}_s \end{pmatrix} = \begin{pmatrix} \boldsymbol{M}_h & \boldsymbol{M}_e \\ \boldsymbol{M}_e & \boldsymbol{K}_s \end{pmatrix} \begin{pmatrix} \boldsymbol{\tau} \\ \boldsymbol{E} \end{pmatrix} = \mathscr{M} \begin{pmatrix} \boldsymbol{\tau} \\ \boldsymbol{E} \end{pmatrix}, \tag{2.1}$$

which acts as an effective boundary condition on the quasi-neutral bulk fluid, where $\boldsymbol{K}_s$ is a tensorial surface conductivity and $\boldsymbol{j}_s$ is the surface current density (in excess of the extrapolated bulk current density, integrated over the interface). Using matched asymptotic expansions (Chu & Bazant 2007), (2.1) can be derived by considering a semi-infinite quasi-equilibrium electrolyte and solving for the velocity $\boldsymbol{u}_s$ and current $\boldsymbol{j}_s$ 'at infinity' relative to the interfacial thickness, e.g. $\lambda = \max\{\lambda_D, L\}$ for a periodic texture of period L or a (non-fractal) random texture with correlation length L.

Following Bazant & Vinogradova (2008), we note some basic physical constraints on $\mathscr{M}$. In most cases, we expect $\mathscr{M}$ to be symmetric, as assumed in (2.1), by analogy with Onsager's relations in (bulk) non-equilibrium thermodynamics (Groot & Mazur 1962). This hypothesis for $\boldsymbol{M}_h$ has been established for Stokes flows over a broad class of patterned surfaces (Kamrin, Bazant & Stone 2009). Here, we focus on $\boldsymbol{M}_e$ by calculating the anisotropic electro-osmotic flow in response to an applied electric field, but according to (2.1) the same tensor also provides the 'streaming surface current' $\boldsymbol{j}_s = \boldsymbol{M}_e \boldsymbol{\tau}$ in response to an applied shear stress. The mobility $\boldsymbol{M}$ is positive definite for a passive surface, which does no work on the fluid. In general, $\boldsymbol{M}_h$, $\boldsymbol{M}_e$ and $\boldsymbol{K}_s$ could be represented by 3×3 matrices to allow for normal flux of fluid (or charge) into a porous (or conducting) surface, driven by normal electric fields (or tensile stresses), but here we consider only insulating, impermeable surfaces, with 2×2 matrices diagonalized by a rotation:

$$\boldsymbol{M}_e = \boldsymbol{S}_\theta \begin{pmatrix} M_e^{\parallel} & 0 \\ 0 & M_e^{\perp} \end{pmatrix} \boldsymbol{S}_{-\theta}, \qquad \boldsymbol{S}_\theta = \begin{pmatrix} \cos\theta & \sin\theta \\ -\sin\theta & \cos\theta \end{pmatrix}. \tag{2.2}$$

Once the orthogonal eigen-directions $\theta = 0, \pi/2$ are identified, the problem reduces to computing the two eigenvalues, $M_e^{\parallel}$ and $M_e^{\perp}$, which attain the maximal and minimal directional mobilities, respectively.

2.2. *Weakly charged, nano-scale striped patterns*

To highlight effects of anisotropy, we focus on flat patterned SH surfaces consisting of periodic stripes, where the surface charge density q and the local (scalar) slip length b vary only in one direction. In the case of thin channels ($h \ll L$), striped surfaces provide rigorous upper and lower bounds on the effective slip (eigenvalues of $\boldsymbol{M}_h$) over all possible two-phase patterns (Feuillebois, Bazant & Vinogradova 2009); for thick channels, sinusoidal stripes also bound the effective slip for arbitrary perturbations in surface height and/or slip length (Kamrin *et al.* 2009). Striped SH surfaces have also been used for drag reduction in pressure-driven flows (Ou & Rothstein 2005), with a typical geometry sketched in figure 1(*a*) corresponding to Cassie's state of a roughly flat liquid surface over gas bubbles trapped in wells. By symmetry, the eigen-directions of $\boldsymbol{M}_e$, $\boldsymbol{M}_h$ and $\boldsymbol{K}_s$ for a striped surface correspond to longitudinal

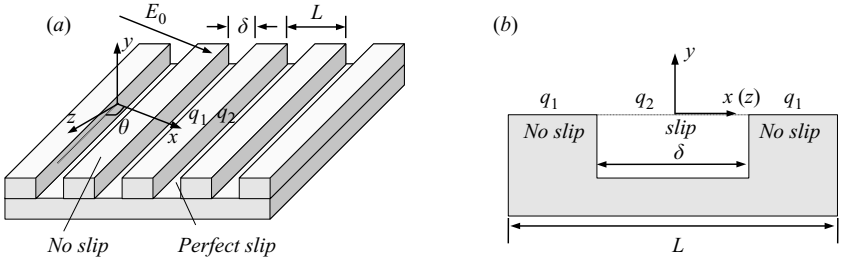

FIGURE 1. (*a*) Sketch of SH stripes: $\theta = \pi/2$ corresponds to transverse, whereas $\theta = 0$ corresponds to longitudinal stripes. (*b*) Situation in (*a*) is approximated by a periodic cell of size L, with equivalent flow boundary conditions on gas/liquid and solid/liquid interface.

($\theta = 0$) and transverse ($\theta = \pi/2$) alignment with the applied electric field or shear stress, so we need only to compute the eigenvalues for these cases using (2.2).

We consider a semi-infinite electrolyte in the region $y > 0$ above a flat patterned surface of period L at $y = 0$ subject to an electric field E_0 in the x direction. The electrostatic potential is given by $\phi(x, y, z) = -E_0 x + \psi(x, y, z)$, where ψ is the perturbation due to diffuse charge. For nano-scale patterns ($L < 1\,\mu$m), we can neglect convection ($Pe = \langle q \rangle E_0 L/\eta\kappa D \ll 1$ for a typical ionic diffusivity D) so that $\psi(x, y, z)$ is independent of the fluid flow. We also assume weak fields $|E_o|L \ll |\psi|$ and weakly charged surfaces ($|\psi| \ll kT/ze = 25/z$ mV at room temperature) for a $z : z$ electrolyte, so that ψ satisfies the Debye–Hückel equation with a boundary condition of prescribed surface charge

$$\Delta\psi = \frac{\partial^2\psi}{\partial x^2} + \frac{\partial^2\psi}{\partial y^2} + \frac{\partial^2\psi}{\partial z^2} = \kappa^2\psi, \qquad -\varepsilon\frac{\partial\psi}{\partial y}(x, 0, z) = q(x, z), \tag{2.3}$$

where $\kappa = \lambda_D{}^{-1} = (2z^2e^2n_\infty/\varepsilon KT)^{1/2}$ is the inverse screening length. In this limit, we can neglect surface conduction (which tends to reduce electro-osmotic flow) compared with bulk conduction ($Du = |\boldsymbol{j}_s|/\sigma E_0 L \ll 1$), so we will only discuss the tensors $\boldsymbol{M}_e$ and $\boldsymbol{M}_h$.

For transverse stripes, $q = q(x) = q(x + L)$, we expand $q(x)$ in a Fourier series

$$q(x) = \langle q \rangle + \sum_{n=1}^{\infty}(A_n\sin(\lambda_n x) + B_n\cos(\lambda_n x)), \tag{2.4}$$

where $\langle q \rangle$ is the mean surface charge, and solve (2.3) by separation of variables

$$\psi = \psi(x, y) = \frac{\langle q \rangle}{\varepsilon\kappa}\mathrm{e}^{-\kappa y} + \sum_{n=1}^{\infty}\frac{1}{\varepsilon\sqrt{\kappa^2 + \lambda_n^2}}(A_n\sin(\lambda_n x) + B_n\cos(\lambda_n x))\mathrm{e}^{-\sqrt{\kappa^2+\lambda_n^2}\,y}, \tag{2.5}$$

where $\lambda_n = 2n\pi/L$. For longitudinal stripes, $q = q(z) = q(z + L)$, the potential $\psi = \psi(y, z)$ has exactly the same form (2.5) with x replaced by z.

The fluid flow satisfies Stokes' equations with an electrostatic body force

$$\eta\Delta\boldsymbol{u} = -\varepsilon\Delta\psi\nabla\phi + \nabla p, \quad \nabla\cdot\boldsymbol{u} = 0. \tag{2.6a, b}$$

To describe the local hydrodynamic slip, we apply Navier's boundary condition

$$\boldsymbol{u}(x, 0, z) = b(x, z)\frac{\partial\boldsymbol{u}}{\partial y}(x, 0, z), \qquad \hat{\boldsymbol{y}}\cdot\boldsymbol{u}(x, 0, z) = 0. \tag{2.7}$$

Far from the surface, $\boldsymbol{u}$ approaches the effective, electro-osmotic 'slip' velocity $\lim_{y\to\infty}\boldsymbol{u}(x, y, z)=\boldsymbol{u}_0$, and the derivatives of $\boldsymbol{u}$ remain bounded. By definition, the flow is two-dimensional in the eigen-directions of the surface.

For transverse stripes, we have $\boldsymbol{u}=(u(x, y), v(x, y), 0)$, $u(x, 0)=b(x)u_y(x, 0)$ and $v(x, 0)=0$. Assuming constants η and ε and using (2.3), we can write (2.6) as

$$\Delta\boldsymbol{u}(x, y) = -\frac{\varepsilon\kappa^2}{\eta}\psi(x, y)\nabla\phi(x, y) + \frac{1}{\eta}\nabla p, \tag{2.8}$$

where the pressure can be eliminated by taking the curl of both sides:

$$\Delta\big(\nabla\times\boldsymbol{u}\big) = -\frac{\varepsilon\kappa^2}{\eta}(E_0\hat{\mathbf{x}}\times\nabla\psi).$$

Taking another curl of this equation and using incompressibility, we obtain

$$\nabla^4 u = \frac{\varepsilon\kappa^2 E_0}{\eta}\left(\frac{\partial^2\psi}{\partial y^2}+\frac{\partial^2\psi}{\partial z^2}\right), \tag{2.9}$$

where $\nabla^4\psi=\kappa^4\psi$ from (2.3). The general solution to (2.9) for $u(x, y)$ has the form

$$u(x, y) = u_0 + \sum_{n=1}^{\infty}(P_n\sin(\lambda_n x) + Q_n\cos(\lambda_n x))\mathrm{e}^{-\lambda_n y} + \frac{\varepsilon E_0}{\kappa^2\eta}\frac{\partial^2\psi}{\partial y^2}, \tag{2.10}$$

where P_n, Q_n are unknown coefficients and the last term involving $\psi(x, y)$ can be obtained from (2.5). The slip boundary condition then determines the coefficients $\{P_n, Q_n\}$ and the electro-osmotic slip $u_0=M_e^{\perp}E_o$.

For longitudinal stripes, the flow is also two-dimensional: $\boldsymbol{u}=(0, v(y, z), u(y, z))$, $u(0, z)=b(z)u_y(0, z)$ and $v(0, z)=0$, where u is again the tangential velocity. Similar steps lead to (2.9) for $u(y, z)$, using (2.3) with $\psi=\psi(y, z)$. The general solution now takes the form

$$u(y, z) = u_0 + \sum_{n=1}^{\infty}(P_n\sin(\lambda_n z) + Q_n\cos(\lambda_n z))\mathrm{e}^{-\lambda_n y} + \frac{\varepsilon E_0}{\eta}\psi, \tag{2.11}$$

where $\{P_n, Q_n\}$ and $u_0=M_e^{\parallel}E_o$ are determined by the slip boundary condition.

3. Striped super-hydrophobic surfaces

3.1. *Hydrodynamic mobility tensor*

To illustrate the theory, we consider an idealized, flat, periodic, charged, striped SH surface in the Cassie state sketched in figure 1(*a*), where the liquid–solid interface has no slip ($b_1=0$) and the liquid–gas interface has perfect slip ($b_2=\infty$). Let ϕ_1 and $\phi_2=\delta/L$ be the area fractions of the solid and gas phases with $\phi_1+\phi_2=1$. Our results apply to a single surface in a thick channel ($h\gg\max\{\lambda_D, L\}$) where effective hydrodynamic slip is determined by flow at the scale of roughness (Bocquet & Barrat 2007), but not to thin channels ($h\ll\min\{\lambda_D, L\}$) where the effective slip scales with the channel width (Feuillebois *et al.* 2009).

Pressure-driven flow past stick-slip stripes has been analysed and shown to depend on the direction of the flow (Lauga & Stone 2003; Cottin-Bizonne *et al.* 2004; Sbragaglia & Prosperetti 2007). Following Bazant & Vinogradova (2008), the

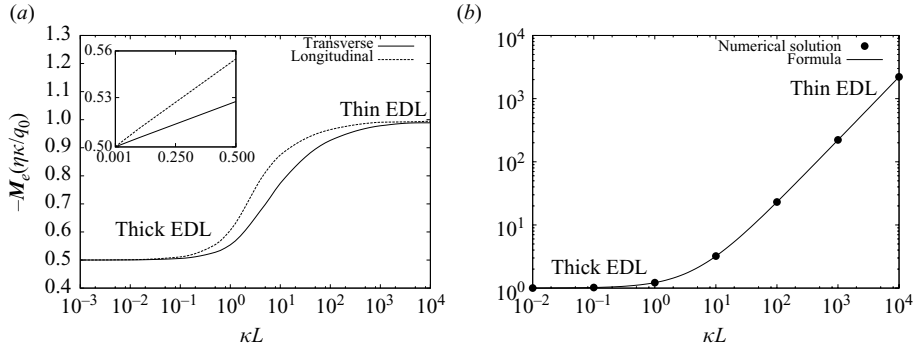

FIGURE 2. Eigenvalues of the electro-osmotic slip tensor $\boldsymbol{M}_e$ for stick-slip stripes of period L and slipping area fraction $\delta/L = 1/2$ as a function of the ratio κL of the period to the electric double-layer (EDL) thickness. Numerical solutions are compared with exact results in the text for the limits $\kappa L \to 0, \infty$ for (a) an uncharged slipping interface $q_1 = q_0$, $q_2 = 0$, with thick EDL limit clarified in the inset, and (b) a surface of constant charge $q_1 = q_2 = q_0$.

hydrodynamic slip tensor $\boldsymbol{M}_h$ must have the form (2.2), where the eigenvalues are

$$M_h^{\perp} = \frac{b_{eff}}{\eta} = \frac{L}{2\pi\eta}\ln\left[\sec\left(\frac{\pi\phi_2}{2}\right)\right] \quad \text{and} \quad M_h^{\parallel} = 2M_h^{\perp}. \tag{3.1}$$

The effective slip for parallel stripes, $M_h^{\parallel}$, is twice that of perpendicular stripes, $M_h^{\parallel}$ (which holds for general grooved surfaces (Kamrin, Bazant & Stone 2009)), just as a vertically oriented elongated body sedimenting due to its own weight falls twice faster than if it were oriented horizontally (Batchelor 1970).

3.2. *Electro-osmotic mobility tensor*

1. *Transverse stripes.* For $\theta = 0$, the region $|x| \leqslant \delta/2$ has $b = \infty$ (i.e. $u_y(x, 0) = 0$) and $q = q_1$, while the region $\delta/2 < |x| \leqslant L/2$ has $b = 0$ and $q = q_2$. Imposing these boundary conditions on the general solution (2.10) yields a dual cosine series

$$\frac{\langle q\rangle E_0}{\eta} + \sum_{n=1}^{\infty}\left(\lambda_n Q_n + \frac{\gamma_n^2 E_0 B_n}{\eta\kappa^2}\right)\cos(\lambda_n x) = 0, \quad \forall\ |x| \leqslant \tfrac{1}{2}\delta, \tag{3.2a}$$

$$u_0 + \frac{\langle q\rangle E_0}{\eta\kappa} + \sum_{n=1}^{\infty}\left(Q_n + \frac{\gamma_n E_0 B_n}{\eta\kappa^2}\right)\cos(\lambda_n x) = 0, \quad \forall\ \tfrac{1}{2}\delta < |x| \leqslant \tfrac{1}{2}L, \tag{3.2b}$$

where $\gamma_n = \sqrt{\lambda_n^2 + \kappa^2}$. (The sine terms vanish due to symmetry.)

For the general case $q_1 \neq q_2$, the dual series can be solved numerically for $M_e^{\perp} = u_0/E_0$ (see figure 2) by truncating the series and taking the inner products with 1 and $\cos(\lambda_n x)$, but exact results are possible in the thin and thick EDL limits. (Below, we also give an exact solution to any value of κL in the case $q_1 = q_2$.) In the thin EDL limit, $\lambda_n/\kappa \to 0$, we have $\gamma_n/\kappa \to 1$. Since B_n are Fourier cosine coefficients of $q(x)$, the dual series can be written as

$$\sum_{n=1}^{\infty}\lambda_n Q_n\cos(\lambda_n x) = -\frac{q_2 E_0}{\eta}, \quad \forall\ |x| \leqslant \tfrac{1}{2}\delta, \tag{3.3a}$$

$$\left(u_0 + \frac{q_1 E_0}{\eta\kappa}\right) + \sum_{n=1}^{\infty} Q_n\cos(\lambda_n x) = 0, \quad \forall\ \tfrac{1}{2}\delta < |x| \leqslant \tfrac{1}{2}L. \tag{3.3b}$$

This dual series can be solved exactly (Sneddon 1966) to obtain

$$M_e^{\perp,thin} = \frac{u_0}{E_0} = -\frac{q_1 + 2q_2\kappa b_{eff}}{\eta\kappa}. \tag{3.4}$$

In the thick EDL limit, $\lambda_n/\kappa \gg 1$, the dual series (3.2) takes the form

$$\sum_{n=1}^{\infty} \lambda_n \Big(Q_n + \frac{\gamma_n E_0 B_n}{\eta\kappa^2} \Big) \cos(\lambda_n x) = -\frac{E_0}{2\eta}(\langle q \rangle + q_2), \quad \forall\ |x| \leqslant \tfrac{1}{2}\delta, \tag{3.5a}$$

$$u_0 + \frac{\langle q \rangle E_0}{\eta\kappa} + \sum_{n=1}^{\infty} \Big(Q_n + \frac{\gamma_n E_0 B_n}{\eta\kappa^2} \Big) \cos(\lambda_n x) = 0, \quad \forall\ \tfrac{1}{2}\delta < |x| \leqslant \tfrac{1}{2}L, \tag{3.5b}$$

which can again be solved exactly to obtain the thick-DL electro-osmotic mobility

$$M_e^{\perp,thick} = \frac{u_0}{E_0} = -\frac{\langle q \rangle}{\eta\kappa} \left[1 + \left(\frac{\langle q \rangle + q_2}{\langle q \rangle} \right) b_{eff}\kappa \right]. \tag{3.6}$$

2. *Longitudinal stripes.* Rotating the SH surface by $\theta = \pi/2$, the region $|z| \leqslant \delta/2$ has $b = \infty$ and $q = q_1$, while the region $\delta/2 < |z| \leqslant L/2$ has $b = 0$ and $q = q_2$. Applying boundary conditions to (2.11), we obtain another dual cosine series

$$\frac{\langle q \rangle E_0}{\eta} + \sum_{n=1}^{\infty} \Big(\lambda_n Q_n + \frac{E_0 B_n}{\eta} \Big) \cos(\lambda_n z) = 0, \quad \forall\ |z| \leqslant \tfrac{1}{2}\delta, \tag{3.7a}$$

$$u_0 + \frac{\langle q \rangle E_0}{\eta\kappa} + \sum_{n=1}^{\infty} \Big(Q_n + \frac{E_0 B_n}{\eta\gamma_n} \Big) \cos(\lambda_n z) = 0, \quad \forall\ \tfrac{1}{2}\delta < |z| \leqslant \tfrac{1}{2}L, \tag{3.7b}$$

which can be solved numerically (figure 2) or exactly for thin and thick EDL. In the thin EDL limit, $\gamma_n/\kappa \to 1$, the dual series (3.7) can be simplified using the $q(x)$ series to obtain again (3.3) and, thus,

$$M_e^{\parallel,thin} = M_e^{\perp,thin} = M_e^{thin} = -\frac{q_1 + 2q_2\kappa b_{eff}}{\eta\kappa}. \tag{3.8}$$

Therefore, we find that the electro-osmotic mobility tensor is isotropic in the thin DL limit, $\boldsymbol{M}_e^{thin} = M_e^{thin}\boldsymbol{I}$, consistent with the examples of Squires (2008). In general, $\boldsymbol{M}_e$ must be isotropic for any flat patterned surface in the thin DL limit, since the effective EO slip velocity is equal to the surface-averaged EO slip velocity (Ramos *et al.* 2003), and thus always in the direction of $\boldsymbol{E}_0$.

In the thick EDL limit, we have $\lambda_n/\gamma_n \to 1$, $\lambda_n/\kappa \gg 1$, and the dual series reduces to

$$\sum_{n=1}^{\infty} \lambda_n \Big(Q_n + \frac{E_0 B_n}{\gamma_n \eta} \Big) \cos(\lambda_n z) = -\frac{\langle q \rangle E_0}{\eta}, \quad \forall\ |z| \leqslant \tfrac{1}{2}\delta, \tag{3.9a}$$

$$\Big(u_0 + \frac{\langle q \rangle E_0}{\eta\kappa} \Big) + \sum_{n=1}^{\infty} \Big(Q_n + \frac{E_0 B_n}{\eta\gamma_n} \Big) \cos(\lambda_n z) = 0, \quad \forall\ \tfrac{1}{2}\delta < |z| \leqslant \tfrac{1}{2}L, \tag{3.9b}$$

which can be solved exactly

$$M_e^{\parallel,thick} = -\frac{\langle q \rangle}{\eta\kappa} \left(1 + 2\kappa b_{eff} \right). \tag{3.10}$$

Since $M_e^{\perp,thick} \neq M_e^{\parallel,thick}$, we see that $\boldsymbol{M}_e$ becomes anisotropic for thick DL.

4. Discussion

4.1. *Uncharged liquid–gas interface*

It is instructive to set the charge to zero on the slipping surface, $q_2 = 0$, to describe the Cassie state of an SH surface with an uncharged liquid–gas interface. The EO flow is then related only to the charge $q_1 = q_0$ on the no-slip liquid–solid interface. First, we consider the thin EDL limit, where the EO mobility is generally isotropic as noted above. Using (3.8), we obtain the simple result of Squires (2008):

$$\boldsymbol{M}_e^{thin} = M_e^{thin}\boldsymbol{I}, \quad \text{where} \quad M_e^{thin} = -\frac{q_0}{\eta\kappa} = -\frac{\langle q\rangle}{\phi_1\eta\kappa}, \tag{4.1}$$

where the EO mobility is the same as that for a homogeneous, solid no-slip surface with charge density q_0, regardless of the orientation or area fraction of the slipping stripes. In other words, there is no EO flow enhancement due to the slipping regions. As explained by Squires (2008), the liquid appears to slip on the charged liquid–solid interface by electro-osmosis, but without any retarding shear stress or amplifying electro-osmotic flow on the uncharged, perfectly slipping liquid–gas interface.

The flow is anisotropic for any finite EDL thickness, and in this case, there is a simple relationship between the electro-osmotic and hydrodynamic mobility tensors in the thick EDL limit. Using (3.6) and (3.10) for the EO mobility eigenvalues and comparing with (3.1), we find

$$\boldsymbol{M}_e^{thick} = -\langle q\rangle\left(\frac{\boldsymbol{I}}{\eta\kappa} + \boldsymbol{M}_h\right) = -\frac{\langle q\rangle}{\eta\kappa}\left(\boldsymbol{I} + \kappa\boldsymbol{b}\right), \tag{4.2}$$

which is a natural tensorial generalization of the classical formula (1.1). In the limit $\kappa L \to 0$ (similar to the thick channel limit), hydrodynamic slip becomes negligible, and the EO flow is isotropic and driven by the average surface charge, $M_e^{thick} \to -\langle q\rangle/\eta\kappa$.

From the thick EDL results of this case we see that the EO velocities are even smaller than in the case of thin EDL. Even if (4.1) is used for $\kappa L \approx 1$, the EO mobility of the SH surface is still smaller than having a constant charge on the surface without any slipping regions. This is consistent with the molecular dynamics simulations of Huang *et al.* (2008) for perpendicular stripes for 1 M NaCl solution confined in parallel walls with no charge on the liquid–gas interface, which also showed no enhancement of the EO flow. Since the effective slip length depends on the pattern, however, some flow enhancement may be possible for thick EDL, even with an uncharged liquid–gas interface, provided that effective slip length is quite large.

4.2. *Charged liquid–gas interface*

The situation is very different if the slipping regions carry some net charge. There is growing evidence that the air–water interface contains an excess of either adsorbed OH^- ions (Shchekin & Borisov 2005; Takahashi 2005; Zangi & Engberts 2005) or H_3O^+ ions (Jungwirth & Tobias 2006; Buch *et al.* 2007). However, electrostatic forces on these mobile ions are balanced by opposite forces on their screening clouds, and we have neglected the resulting interfacial torque due to the low gas viscosity. Instead, the diffuse charge in our model screens the fixed charge of solid surfaces below the gas bubble, which could, in principle, be controlled, as in electrowetting of SH surfaces (Krupenkin *et al.* 2004).

To quantify the possible EO flow enhancement, we consider the special case of uniform surface charge $q_1 = q_2 = q_0$. In this case, an exact solution is possible for

arbitrary EDL thickness and any stripe orientation:

$$\boldsymbol{M}_e = M_e \boldsymbol{I}, \quad \text{where} \quad M_e = -q_0 \left(\frac{1}{\eta\kappa} + M_h^{\parallel} \right) = -\frac{q_0}{\eta\kappa}(1 + 2b_{eff}\kappa). \tag{4.3}$$

Clearly, a large EO flow enhancement, similar to that of an isotropic surface (1.1), is possible with a charged liquid–gas interface (figure 2*b*). This conclusion holds even if the charge is not homogeneous. For thin EDL $\kappa L \sim 10^3$, and $q_2/q_1 \sim 0.1 - 1$, $\phi_2 \sim 0.5$, the theory predicts EO flow enhancement by factor of 10–100. For thick EDL, this factor approaches 1, but is offset by the prefactor κ^{-1} in the case of constant charge. We conclude that SH electrokinetic enhancement is possible with a charged liquid–gas interface, perhaps by an order of magnitude, versus a homogeneous no-slip surface.

5. Conclusion

We have analysed electro-osmotic flows over patterned surfaces of non-uniform charge and local slip length. Unlike the approach of Squires (2008), we have obtained general solutions to arbitrary EDL thickness, surface charge distribution and slip variation, which are qualitatively different from the thin EDL limit. We have shown that the electrokinetic response of a patterned slipping surface is generally anisotropic and describable by a third rank interfacial mobility tensor (2.1), analogous to the tensorial linear response of a thin microchannel (Ajdari 2001). For stick-slip stripes, we have calculated the electro-osmotic mobility tensor and shown that it is not simply related to the hydrodynamic mobility tensor (Bazant & Vinogradova 2008). In particular, a tensorial generalization (4.2) of the classical formula (1.1) does not hold, except for uncharged slipping regions.

Our results provide some guidance for the design of SH surfaces for electrokinetic applications. For an uncharged liquid–gas interface with thick EDL, our results are closely related to those of Lauga & Stone (2003) for pressure-driven flows, since EO flow enhancement is directly set by the hydrodynamic mobility tensor. For an uncharged liquid–gas interface with thin EDL, we also confirm the result of Squires (2008) that there is no enhancement of EO flow, but the general response for an SH surface can be quite different. Our main conclusion is that a charged liquid–gas interface is required to achieve significant enhancement of EO flow. For a uniformly charged SH surface, we show that the EO mobility (4.3) is isotropic and can exhibit large enhancement from hydrodynamic slip, possibly by an order of magnitude.

This research was supported by the National Science Foundation under Contract DMS-0707641 (M.Z.B.).

REFERENCES

Ajdari, A. 2001 Transverse electrokinetic and microfluidic effects in micropatterned channels: lubrication analysis for slab geometries. *Phys. Rev.* E **65**, 016301.

Ajdari, A. & Bocquet, L. 2006 Giant amplification of interfacially driven transport by hydrodynamic slip: diffusio-osmosis and beyond. *Phys. Rev. Lett.* **96**, 186102.

Batchelor, G. K. 1970 Slender-body theory for particles of arbitrary cross-section in stokes flow. *J. Fluid Mech.* **44**, 419–440.

Bazant, M. Z. & Vinogradova, O. I. 2008 Tensorial hydrodynamic slip. *J. Fluid Mech.* **613**, 125–134.

Bocquet, L. & Barrat, J. L. 2007 Flow boundary conditions from nano- to micro-scales. *Soft Matter* **3**, 685–693.

Buch, V., Milet, A., Vácha, R., Jungwirth, P. & Devlin, J. P. 2007 Water surface is acidic. *PNAS* **104**, 7342.

Chu, K. T. & Bazant, M. Z. 2007 Surface conservation laws at microscopically diffuse interfaces. *J. Colloid Interface Sci.* **315**, 319–329.

Cottin-Bizonne, C., Barentin, C., Charlaix, E., Bocquet, L. & Barrat, J. L. 2004 Dynamics of simple liquids at heterogeneous surfaces: molecular-dynamic simulations and hydrodynamic description. *Eur. Phys. J.* E **15**, 427.

Cottin-Bizonne, C., Barrat, J. L., Bocquet, L. & Charlaix, E. 2003 Low-friction flows of liquid at nanopatterned interfaces. *Nat. Mater.* **2**, 237–240.

Cottin-Bizonne, C., Cross, B., Steinberger, A. & Charlaix, E. 2005 Boundary slip on smooth hydrophobic surfaces: intrinsic effects and possible artifacts. *Phys. Rev. Lett.* **94**, 056102.

Feuillebois, F., Bazant, M. Z. & Vinogradova, O. I. 2009 Effective slip over superhydrophobic surfaces in thin channels. *Phys. Rev. Lett.* **102**, 026001.

Groot, S. R. De & Mazur, P. 1962 *Non-Equilibrium Thermodynamics*. Interscience.

van der Heyden, F. H. J., Bonthuis, D. J., Stein, D., Meyer, C. & Dekker, C. 2006 Electrokinetic energy conversion efficiency in nanofluidic channels. *Nano Lett.* **6**, 2232–2237.

Huang, D. M., Cottin-Bizzone, C., Ybert, C. & Bocquet, L. 2008 Massive amplification of surface-induced transport at superhydrophobic surfaces. *Phys. Rev. Lett.* **20**, 092105.

Joly, L., Ybert, C., Trizac, E. & Bocquet, L. 2004 Hydrodynamics within the electric double layer on slipping surfaces. *Phys. Rev. Lett.* **93**, 257805.

Joseph, P., Cottin-Bizonne, C, Benoĭt, J. M., Ybert, C., Journet, C., Tabeling, P. & Bocquet, L. 2006 Slippage of water past superhydrophobic carbon nanotube forests in microchannels. *Phys. Rev. Lett.* **97**, 156104.

Jungwirth, P. & Tobias, D. J. 2006 Specific ion effects at the air/water interface. *Chem. Rev.* **106**, 1259–1281.

Kamrin, K., Bazant, M. Z. & Stone, H. A. 2009 Effective slip boundary conditions for arbitrary periodic surfaces: The surface mobility tensor, arXiv: 0911.1328.

Khair, A. S. & Squires, T. M. 2009 The influence of hydrodynamic slip on the electrophoretic mobility of a spherical colloidal particle. *Phys. Fluids* **21**, 042001.

Krupenkin, T. N., Taylor, J. A., Schneider, T. M. & Yang, S. 2004 From rolling ball to complete wetting: the dynamic tuning of liquids on nanostructured surfaces. *Langmuir* **20**, 3824–3827.

Lauga, E., Brenner, M. P. & Stone, H. A. 2007 *Handbook of Experimental Fluid Dynamics*, chap. 19, pp. 1219–1240. Springer.

Lauga, E. & Stone, H. A. 2003 Effective slip in pressure-driven stokes flow. *J. Fluid Mech.* **489**, 55–77.

Muller, V. M., Sergeeva, I. P., Sobolev, V. D. & Churaev, N. V. 1986 Boundary effects in the theory of electrokinetic phenomena. *Colloid J. USSR* **48**, 606–614.

Ou, J. & Rothstein, J. P. 2005 Direct velocity measurements of the flow past drag-reducing ultrahydrophobic surfaces. *Phys. Fluids* **17**, 103606.

Ramos, A., González, A., Castellanos, A., Green, N. G. & Morgan, H. 2003 Pumping of liquids with AC voltages applied to asymmetric pairs of microelectrodes. *Phys. Rev.* E **67**, 056302.

Sbragaglia, M. & Prosperetti, A. 2007 A note on the effective slip properties. *Phys. Fluids* **19**, 043603.

Shchekin, A. K. & Borisov, V. V. 2005 Thermodynamics of nucleation on the particles of salts-strong electrolytes: the allowance for ion adsorption in the droplet surface layer. *Colloid J.* **67**, 774–787.

Sneddon, I. N. 1966 *Mixed Boundary Value Problems in Potential Theory*. North-Holland.

Squires, T. M. 2008 Electrokinetic flows over inhomogeneously slipping surfaces. *Phys. Fluids* **20**, 092105.

Squires, T. M. & Quake, S. R. 2005 Microfluidics: fluid physics at the nanoliter scale. *Rev. Mod. Phys.* **77**, 977.

Stone, H. A., Stroock, A. D. & Ajdari, A. 2004 Engineering flows in small devices. *Annu. Rev. Fluid Mech.* **36**, 381–411.

Takahashi, M. 2005 ζ potential of microbubbles in aqueous solutions: electrical properties of the gas–water interface. *J. Phys. Chem.* B **109**, 21858–21864.

Vinogradova, O. I. 1995 Drainage of a thin liquid film confined between hydrophobic surfaces. *Langmuir* **11**, 2213.

Vinogradova, O. I. 1999 Slippage of water over hydrophobic surfaces. *Intl J. Miner. Proc.* **56**, 31–60.

Vinogradova, O. I., Bunkin, N. F., Churaev, N. V., Kiseleva, O. A., Lobeyev, A. V. & Ninham, B. W. 1995 Submicrocavity structure of water between hydrophobic and hydrophilic walls as revealed by optical cavitation. *J. Colloid Interface Sci.* **173**, 443–447.

Vinogradova, O. I., Koynov, K., Best, A. & Feuillebois, F. 2009 Direct measurements of hydrophobic slippage using double-focus fluorescence cross-correlation. *Phys. Rev. Lett.* **102**, 118302.

Vinogradova, O. I. & Yakubov, G. E. 2003 Dynamic effects on force measurements. 2. Lubrication and the atomic force microscope. *Langmuir* **19**, 1227–1234.

Zangi, R. & Engberts, J. B. F. N. 2005 Physisorption of hydroxide ions from aqueous solution to a hydrophobic surface. *J. Am. Chem. Soc.* **127**, 2272–2276.